Mutational Effects at the Subunit Interfaces of Human Hemoglobin: Evidence for a Unique Sensitivity of the T Quaternary State to Changes in the Hinge Region of the α1β2 Interface†

Robert W. Noble,* Hilda L. Hui, Laura D. Kwiatkowski, Paul Paily, Alice DeYoung, Anita Wierzba, and Judith E. Colby

Department of Medicine, University at Buffalo, Veterans Administration Medical Center, Buffalo, New York 14215

Stefano Bruno‡ and Andrea Mozzarelli‡,§

Institute of Biochemical Sciences and Italian Institute for the Physics of Matter, University of Parma, 43100 Parma, Italy

Received May 15, 2001; Revised Manuscript Received August 21, 2001

ABSTRACT: A set of variant human hemoglobins, each with an Ala or Gly substitution at a single residue, has been prepared, and the kinetics of their reactions with carbon monoxide have been measured. This reaction is rate-limited by the binding of the first CO to the deoxygenated T state of the protein. The magnitudes of the effects of the mutations on CO combination vary widely, and, with the exception of βY145, the residues with the most significant effects on these kinetics are found in the hinge region of the α1β2 interface. Mixed-metal hybrids, with zinc protoporphyrin IX in place of heme on both α or both β subunits, were prepared for βW37E, βW37A, αY140G, and αY140A, hinge region variants causing large kinetic changes, and for βY145G. Such hybrids permit measurements of the kinetics of CO binding to only the heme-containing α or β subunits within the unliganded hemoglobin tetramer. Mutations at β37 and α140 have global effects on the T state, increasing the rates of CO binding to both types of subunits. Mutation of βY145 has a large effect on the β subunits in the deoxygenated T state, but very little effect on the α subunits. Oxygen equilibria measurements on the crystalline T state of βW37E also indicate large affinity increases in both subunits of this variant. The overall oxygen equilibria of the variant hemoglobins in solution are sensitive to numerous variables besides the properties of the deoxygenated T state. In contrast to CO combination kinetics, the residues whose alterations cause the largest changes in overall oxygen equilibria in solution are scattered seemingly randomly within the α1β2 interface.

Cooperativity in ligand binding and other allosteric effects are the unique property of the intact hemoglobin tetramer, Hb.[1] The isolated α and β chains, as well as αβ dimers, exhibit high ligand affinities without significant cooperativity (*1*−*3*). It is the assembly of two αβ dimers into tetrameric Hb which elicits the functional properties which distinguish this molecule. The overall oxygen affinity is greatly reduced by this assembly, and within the tetramer, ligand binding is accompanied by both structural and functional transitions which result in cooperativity. If the two αβ dimers are denoted α1β1 and α2β2, the chains within the dimers interact through the identical α1β1 and α2β2 interfaces. When two deoxy-αβ dimers combine to produce the deoxyHb tetramer, the only direct contacts between like subunits occur at the α1α2 interface where ionic interactions form between the COOH-terminal residue, Arg141α, of one subunit and residues Asp126α and Lys127α on the opposite α subunit. It is the formation of these contacts together with the formation of contacts along the α1β2 interface (and the symmetry-related α2β1 interface) that is a necessary condition for cooperativity, and it is the α1α2 and α1β2 interfaces that exhibit the greatest structural rearrangement in the course of ligand binding. In contrast to the deoxygenated T state tetramer, which has many intersubunit contacts and appears to have only a single quaternary structure, the fully liganded hemoglobin tetramer is characterized by a range of energetically similar quaternary structures (referred to as the R^e ensemble) that have relatively few intersubunit contacts (*4*). The ligand-induced transition from the deoxygenated T state structure to the structures of the ligand-saturated R^e ensemble involves rotations of the two αβ dimers with respect to one another about axes which pass through the two α chains and

† This work was supported by Program Project Grant PO1 GM58890 from the National Institutes of Health.

* To whom correspondence should be addressed at the Department of Medicine, University at Buffalo, VA Medical Center, Room 202, Building 20, 3495 Bailey Ave., Buffalo, NY 14215. E-mail: rnoble@acsu.buffalo.edu, Phone: (716) 862-6538, FAX: (716) 862-6526.

‡ Institute of Biochemical Sciences.

§ Italian Institute for the Physics of Matter.

[1] Abbreviations: Hb, hemoglobin; HbA, normal human hemoglobin A; IHP, inositol hexaphosphate; bisTris, bis(2-hydroxyethyl)iminotris-(hydroxymethyl)methane; βV1M, recombinant hemoglobin with the Val1β → Met mutation; αL91A, recombinant hemoglobin with the Leu91α → Ala mutation; all other Hb mutants are indicated in the same manner; HbAXL99α, normal human HbA which has been cross-linked between its two α99 lysine residues by reaction with bis(3,5-dibromosalicyl)fumarate; βW37EXL99α, the βW37E variant of HbA cross-linked between its α99 residues.

10.1021/bi010988p CCC: $20.00
Published on Web 09/22/2001

define two regions of the $\alpha 1\beta 2$ interface. The region between the FG corner and C terminus of the α subunit and the C helix of the β subunit lies closest to the rotation axes and is termed the hinge region. The region between the FG corner and the C terminus of the β subunit and the C helix of the α subunit, termed the switch region, lies furthest from the rotation axes and is where the largest motion of the two dimers relative to one another occurs.

To further our understanding of the structural origins of the properties of the hemoglobin tetramer, we have undertaken a systematic examination of the functional consequences of the deletion of the side chains of individual amino acids which contribute to the $\alpha\beta$ interfaces or are suspected of contributing to the linkage between interface and heme. Using site-directed mutagenesis and expression in *E. coli*, a series of variant hemoglobins, each with a single Ala or Gly substitution at an α or β chain residue, has been prepared. Perhaps the most unique property resulting from tetramer assembly is the drastic, several hundredfold, reduction in the affinity of the unliganded or deoxygenated Hb molecule for the binding of the first ligand (*2*). This reduction in ligand affinity is reflected in a large decrease in the rate of CO combination with the unliganded, tetrameric protein (*3*). Therefore, the kinetics of CO combination with each variant have been examined. For five variants, the functional properties of the T quaternary state were also assessed by measurement of oxygen binding equilibria of T state crystals. In addition, for most of the variants, preliminary measurements of overall oxygen equilibria in solution were carried out using tonometric procedures.

EXPERIMENTAL PROCEDURES

Native human HbA was prepared from freshly drawn blood and was stripped of endogenous organic phosphates by passage through a Dintzis deionizing column (*5*) as described by Doyle et al. (*6*). Isolated α and β chains of HbA were prepared by a modification of the Bucci and Fronticelli method (*7*) as described by Hernan et al. (*8*).

Mutagenesis and Overexpression of the β Globin Gene in E. coli. Mutations in the β globin gene were generated by cassette mutagenesis or by PCR mutagenesis using the QuikChange Site-Directed Mutagenesis Kit available from Stratagene (LaJolla, CA). The T7 expression plasmid, pETβ102, described by Hernan et al. (*8*) was used regardless of the mutagenesis procedure employed. This plasmid contains a synthetic β globin gene in which the codon usage has been optimized for expression in *E. coli* and unique restriction endonuclease recognition sites have been incorporated into the coding sequence. Oligonucleotides used for mutagenesis were purchased from BIO-SYNTHESIS (Lewisville, TX) or Integrated DNA Technologies (Coralville, IA). After mutagenesis, plasmids were transformed into DH5α competent cells or the Epicurian Coli XL1-Blue competent cells that come with the QuikChange Kit. Plasmids containing the desired mutations were identified by automated DNA sequencing done at The University of Iowa College of Medicine DNA Core Facility.

T7 expression plasmids were transformed into competent *E. coli* BL21(DE3) purchased from Novagen (Madison, WI). Transformed strains were grown in LB media (1 L of culture per 2.8 L fernbach flask) containing 100 μg/mL ampicillin to an OD_{600} of 1.0, induced with 0.4 mM IPTG, and allowed to incubate at 37 °C with vigorous shaking for 2 h. The bacteria were harvested by centrifugation, and the mutant β globins[2] were purified, reconstituted with heme, and combined with α chains as described by Hernan et al. (*8*).

Mutagenesis of the α Globin Gene and Coexpression of the α and β Globin Genes in E. coli. The αK40G and αY42A mutations were created by cassette mutagenesis using a modified form of pUC18 in which a synthetic α globin gene that uses optimum *E. coli* codons was cloned between the *Xba*I and *Pst*I sites of the polylinker region. The other restriction endonuclease recognition sites in the linker region of this plasmid (which was provided by Drs. Ron Hernan and Steven Sligar, University of Illinois, Champaign−Urbana) were eliminated in order to facilitate cassette mutagenesis. The oligonucleotides that were used to make the mutant cassettes were purchased from BIO-SYNTHESIS (Lewisville, TX). After transformation into competent DH5α cells, automated DNA sequencing done at The University of Iowa College of Medicine DNA Core Facility was used to identify plasmids that contained the αK40G or αY42A mutation. The mutated α globin genes were then cloned into the region between the *Xba*I and *Pst*I sites of the pUC18-based α/β coexpression vector described by Hernan et al. (*8, 9*). The entire α/β globin operon was removed from this pUC18-based coexpression vector and cloned between the *Xba*I and *Hin*dIII sites of the T7 expression plasmid pET17b (Novagen, Madison, WI).

The other α mutations were created by PCR mutagenesis using the QuikChange Kit. The mutations were created using the pET17b-based expression vector described above in which residue 42α was mutated back to tyrosine. The oligonucleotides used as PCR primers were purchased from Integrated DNA Technologies (Coralville, IA). After mutagenesis, plasmids were transformed into DH5α competent cells or the Epicurian Coli XL1-Blue competent cells that come with the QuikChange Kit. Plasmids containing the desired mutations were identified by automated DNA sequencing done at The University of Iowa College of Medicine DNA Core Facility.

Transformed *E. coli* strain BL21(DE3) cells were grown at 37 °C in LB media (1 L of culture per 2.8 L fernbach flask) containing 100 μg/mL ampicillin for 36 h with gentle shaking (~60 rpm). The cells were not induced with IPTG because induction resulted in lower hemoglobin production. The mutant α globins were isolated from the expressed hemoglobin. and functionally homogeneous mutant hemoglobins were assembled from normal human β chains, the α globin, and hemin as described by Hui et al. (*10*).

Cross-Linked Hemoglobins. HbA was cross-linked between its α99 Lys residues essentially by the method of Chatterjee et al. (*11*) and Snyder et al. (*12*) as described by Kwiatkowski et al. (*13*). The cross-linked derivative of a hemoglobin variant was generally prepared by the same procedure used for HbA. An alternative procedure of combining the mutant β globin with heme and cross-linked

[2] In this paper, the term globin refers to the polypeptide of a hemoglobin subunit without a bound porphyrin molecule. A chain is a globin molecule with a bound heme. When a chain is incorporated into a Hb molecule, it is also referred to as a subunit. When a chain contains zinc protoporphyrin IX rather than heme, it is referred to as a Zn chain.

α chain dimers was used in the preparation of the β(W37E)-XL99α variant (*13*). Cross-linked α chains were prepared from cross-linked HbA, HbAXL99α, as previously described by Kwiatkowski et al. (*13*).

α and β Globins of HbA. The globin of human HbA was prepared by the acid acetone precipitation method of Rossi-Fanelli et al. (*14*) as modified and described by Hui et al. (*10*). The precipitated globin was solubilized in 8 M urea, 3 mM DTT in 5 mM phosphate, pH 6.7, buffer and fractionated into its α and β globin components by chromatography in urea buffers on a CM Sepharose CL 6B column by a modification of the method of Clegg et al. (*15*) and described by Hui et al. (*10*). Alternatively, α and β globins were prepared from isolated α and β chains by the same acid acetone method described above.

Human Hemoglobin β Chains Containing Zinc Protoporphyrin IX. β[Zn]chains were prepared by reacting β globin with zinc protoporphyrin IX. The Zn porphyrin was solubilized in ethanol made basic by drops of 1 M Tris base. A 16 mg/mL solution of β globin in 8 M urea, 5 mM phosphate, pH 6.7, buffer was diluted to 0.3 mg/mL in water, and a 1.2 molar excess of Zn porphyrin was added. The pH of the reaction mixture was adjusted to 6.7 and the mixture left at 4 °C overnight. The sample was concentrated through PM30 membranes, and centrifuged at 34800*g* for 20 min. To purify the β[Zn]chains, the reaction mixture was passed through a G 25 column preequilibrated with 10 mM HCl-bisTris, pH 6.5, buffer and loaded onto a CM 52 column equilibrated with the same buffer. β[Zn]chains were eluted from the CM 52 column using 10 mM HCl-bisTris, 50 mM NaCl, pH 6.5. The β[Zn]chains were brought to pH 7 with drops of 1 M Tris, and then were stored in liquid nitrogen until use. From 600 mg of purified β globin, 192 mg of β[Zn]chains were obtained by this procedure. Since Zn porphyrin is light-sensitive, all preparations of and experiments involving Zn porphyrin containing chains or hemoglobins were carried out in very dim light.

Human Hemoglobin α Chains Containing Zinc Protoporphyrin IX. α[Zn]chains were prepared by reacting α globin with zinc protoporphyrin IX. α chains at 12 mg/mL in 8 M urea, 3 mM DTT, 5 mM phosphate buffer, pH 6.7, were diluted to 0.3 mg/mL in water, and a 1.2 molar excess of Zn porphyrin was added. The pH of the reaction mixture was adjusted to 8 by dropwise addition of 1 M Tris base and left at 4 °C overnight. After concentration through PM 30 membranes and centrifugation at 34800*g* for 20 min, α-[Zn]chains were purified by passing the sample through a G25 course column preequilibrated in 15 mM HCl-Tris, pH 8, buffer and then loaded onto a DE 52 column in the same buffer. α[Zn]chains were eluted from the DE 52 column with the starting buffer, and were further purified on the HPLC (Waters 650) using a DEAE Toso Haas column with a gradient from 15 mM HCl-Tris, pH 8.0, to 15 mM HCl-bisTris, pH 7.0, at a flow rate of 5 mL/min in an 85 min run. Unless otherwise indicated, this is the standard HPLC protocol. From 816 mg of α globin, 325 mg of α[Zn]chains (40% yield) were obtained by this method.

α[Zn]chains were also prepared by the heme displacement method. We have found that the incubation of α chains with Zn protoporphyrin IX can result in the complete replacement of heme by the Zn porphyrin, irrespective of ligand bound to the heme groups. α chains at a concentration of 5 mg/mL in 15 mM HCl-Tris buffer, pH 8, were incubated overnight with a 1.5 molar excess of Zn porphyrin at 4 °C. After centrifugation at 38400*g* for 20 min, the sample was passed through a hydrophobic column of phenyl Sepharose (2 × 6 cm) preequilibrated with the same pH 8 buffer. Excess Zn porphyrin and displaced hemin were retained on this column. Two additional rounds of incubation with Zn porphyrin followed by column purification were required to complete the replacement of all hemes with Zn porphyrin. The progress of displacement was followed spectrophotometrically. The α[Zn]chains were put through a final purification step by the standard HPLC protocol. From 136 mg of α[Fe]chains, 40 mg of α[Zn]chains (29% yield) was obtained. Although zinc porphyrin will also replace the heme groups of β chains and intact HbA, the replacement is much less complete than for α chains, and complete replacement cannot be obtained without unacceptable losses.

Zn-containing, cross-linked α chains, α[Zn]XL99, were prepared from cross-linked α chains by the heme displacement procedure as described above for preparing Zn-containing α chains. Unlike the α chains, αXL99 chains required a total of only two rounds of incubation with Zn porphyrin and column purification for complete replacement of the heme groups with Zn porphyrin.

Preparation of Fe−Zn Hybrids of Human HbA. Symmetrical, Fe−Zn hybrids of HbA were assembled by combining a Zn porphyrin containing chain with a 1.2-fold molar excess of its corresponding heme-containing partner chain, α[Zn]chains with β[Fe]chains and α[Fe]chains with β[Zn]-chains. The oxygenated derivatives of the heme-containing partner chains were used rather than the more stable CO derivatives. The conversion of CO derivatives to oxygenated derivatives requires exposure of the heme protein to light (*13*). Since zinc porphyrin is light-sensitive, it was necessary to avoid the need to use this procedure. The resulting hybrid hemoglobins were purified by chromatography on a DE52 column (2 × 6 cm) using a 350 mL gradient from 15 mM HCl-Tris, pH 8.2, to 60 mM HCl-Tris, pH 8.2.

Symmetrical Fe−Zn Hybrids of βW37E. For the βW37E variant, the α[Fe]β[Zn] hybrid was prepared by combining normal α chains with the βW37E globin and Zn protoporphyrin IX. The β globin, at a concentration of approximately 6 mg/mL in 8 M urea, was diluted approximately 20-fold into water, and 1.2 equiv of oxygenated α chains and 1.0 equiv of Zn protoporphyrin per equivalent of β globin were added. The pH was adjusted to 8. Following 1 h of incubation at 4 °C, the dilute product was concentrated with an Amicon PM30 membrane, and purification was carried out by chromatography on a DE52 column as described for the purification of Fe−Zn hybrids of HbA. Since Zn protoporphyrin has the potential to replace heme in α chains, the excess α chains were carefully examined spectrophotometrically for the presence of Zn porphyrin. None was detected. The equivalent cross-linked Fe−Zn hybrid, αXL99[Fe]β-[Zn], was prepared by the same procedure except cross-linked α chain dimers, αXL99, were used in place of normal α chains.

The α[Zn]βW37E[Fe] hybrid and its cross-linked derivative, αXL99[Zn]βW37E[Fe], were prepared essentially as described by Hernan et al. (*8*) and Kwiatkowski et al. (*13*) except that α[Zn] chains and cross-linked αXL99[Zn] chains were used.

Symmetrical Fe−Zn Hybrids of βW37A and βY145G. Uncross-linked Fe−Zn hybrids of these variants were prepared by the same procedures used for the βW37E hybrids.

Fe−Zn Hybrids of αY140G and αY140A. These were prepared by the reciprocal of the procedures used for the hybrids of the two β subunit variants. For the α[Zn]β[Fe] hybrids, the mutant α globins in urea were diluted into water, and a 1.2 molar excess of Zn protoporphyrin IX was added. The pH was adjusted to 8. Following overnight incubation at 4 °C, the resulting αY140G[Zn] or αY140A[Zn] chains were mixed with oxygenated human β chains. After 30 min, the resulting mixtures were concentrated, passed through Phenyl Sepharose columns to remove excess Zn porphyrin, and then fractionated by the standard HPLC protocol. For the α[Fe]β[Zn] hybrids, the αY140G or αY140A globins in urea were again diluted into water, and in this case 1.2 molar excess of cyanohemin was added along with 1.2 molar excess of β[Zn] chains. Following overnight incubation and concentration of the resulting solutions, fractionation was again carried out by HPLC.

The kinetics of CO combination with the deoxygenated hemoglobin tetramers were measured by rapid-mixing, stopped-flow procedures. These measurements were carried out with an OLIS (On Line Instrument Systems, Inc., Bogart, GA) stopped-flow apparatus. The procedures were essentially those of Gibson (*16, 17*) as described by Doyle et al. (*6*). Reactions were followed at 420 and 435 nm using a 1.7 cm path length cell. Concentrations of CO and hemoglobin (in heme equivalents) were generally 20 and 2 μM, respectively.

Kinetic transients were fitted to single or multiple exponential functions using successive integration and Levenberg−Marquardt fitting routines supplied by OLIS and Levenberg−Marquardt fitting routines as supplied in Sigma Plot (SPSS Science).

Since on each symmetrical, FeZn hybrid hemoglobin tetramer there are only two ligand binding sites, with presumably identical properties in the absence of ligand, their combination kinetic transients were fitted to the sequential reaction mechanism in eq 1.

$$\mathrm{Hb} + 2\mathrm{CO} \xrightarrow{2k_1} \mathrm{HbCO} + \mathrm{CO} \xrightarrow{k_2} \mathrm{Hb(CO)_2} \qquad (1)$$

It should be noted that this formulation is not valid if a significant fraction of the hemoglobin is dissociated into αβ dimers.

Oxygen binding isotherms were measured by tonometry by applying the Nagel et al. (*18*) modification of the method of Allen et al. (*19*). A 500 mL tonometer with a 2 mm cuvette attached to it was used. The Hb concentration was approximately 160 μM in heme equivalents. Spectroscopic measurements were carried out with a Cary 14 spectrophotometer modified by OLIS for computer control and on-line data acquisition. To maintain the heme groups in their reduced, ferrous state, the enzyme system of Hayashi et al. (*20*) was utilized.

Kinetic and equilibrium measurements were carried out in a buffer containing 100 mM HCl-bisTris, pH 7. This buffer was prepared by titrating the appropriate amount of HCl with bisTris base to pH 7 followed by adjustment of the solution volume to give the desired chloride concentration. Measurements were carried out in the absence and presence of 100 μM IHP. A solution of the latter was prepared from the sodium salt of IHP (Sigma). The pH of the solution was adjusted by titration with the acid form of Amberlite IR120 resin (*21*).

Oxygen Binding to Crystals of Deoxygenated Hemoglobin. Crystals for microspectrophotometry were grown from PEG 8000 M_r solutions at room temperature as previously described (*22*). Once grown, the crystals were washed sequentially with 20 and 36% (w/v) anaerobic PEG 8000 M_r containing 30 mM sodium dithionite and 10 mM potassium phosphate, pH 7.2, and were stored at 20 °C until used (*22*). These conditions were modified for the preparation of crystals of the βW37E variant by the addition of 1 mM IHP to both the crystal growth and washing buffers.

Crystals were resuspended 1 time in a solution containing 36% (w/v) PEG 8000, 10 mM potassium phosphate, 1 mM EDTA, 30 mM sodium dithionite, pH 7.2, and 6 times in a dithionite-free buffer containing 36% (w/v) PEG 8000, 10 mM potassium phosphate, 3000 units/mL catalase, pH 7. Crystals were anaerobically loaded in the Dvorak−Stotler flow cell (*23*) that was mounted on the thermostated stage of a Zeiss MPM03 microspectrophotometer (*24*). Crystal orientation and polarized absorption measurements were carried out as previously described (*24*).

Polarized absorption spectra were recorded as a function of oxygen pressure. Helium−oxygen mixtures were obtained using an Environics 200 gas mixture generator. Fractional saturation with oxygen and fractional concentration of oxidized hemes were calculated by fitting the observed spectra to the spectra of fully deoxygenated, oxygenated, and oxidized hemoglobin plus a baseline offset (*24*). Individual crystals of βW37E were exposed to only one or two oxygen pressures since the long time required for oxygen equilibration leads to relatively high concentrations of oxidized hemes. Oxygen binding measurements were carried out at 15 °C.

RESULTS AND DISCUSSION

A set of variant Hbs, each with an Ala or Gly substitution at a single sequence position, has been prepared. In all, 27 sequence positions of HbA have been modified in this way. In addition, one double variant (βW37A, N108A) has been produced. The nucleotide sequence of every variant globin gene was determined. The purity of the assembled hemoglobins was assessed by disk gel electrophoresis and by HPLC. The deoxy derivative of every variant hemoglobin, with the exception of βP124A, αR92A, and αP95A, has been crystallized, and its high-resolution structure has been determined. All of the variant subunits are properly folded, and all deoxygenated tetramers exhibit the T quaternary structure.[3] The major issue to be examined in the present article is the effect of these mutations on the low-affinity, deoxygenated T quaternary state of the hemoglobin molecule.

Kinetics of CO Combination with Deoxygenated Hemoglobin Variants. The results of measurements of the kinetics of CO combination with the deoxygenated derivatives of all 35 variants are reported in Table 1 along with the results for HbA, αV1M, and βV1M. Measurements were carried out in pH 7 bisTris buffer in the presence and absence of

[3] Arthur Arnone and Jeffrey Kavanaugh, University of Iowa, personal communication.

Table 1: Rate Constants for CO Combination with Ala and Gly Variants of HbA (20 °C, 0.1 M HCl-bisTris Buffer, pH 7, [Hb] = 2 μM in Heme Equivalents)

variant	rate constant (μM^{-1} s^{-1}) without IHP	rate constant (μM^{-1} s^{-1}) 0.1 mM IHP	effect ratio
	β Chain Variants		
HbA	0.18 A[a]	0.09 A	
β1 Val→Met	0.17 A	0.09 A	1.0
β33 Val→Ala	0.18 A	0.10 A	1.1
β34 Val→Gly	0.31 A	0.15 A	1.7
β35 Tyr→Ala	0.34	0.19 A	2.1
β36 Pro→Ala	3 (6%), 0.4 (94%)	0.24 A	2.7
β37 Trp→Ala	5.4 (26%), 1.1 (74%)	0.75	8.3
β37 Trp→Gly	4.6 (32%), 1.5 (68%)	1.0	11.0
→Gly XL99α[b]	1.3	1.0	11.1
β42 Phe→Ala	0.14 A	0.13 (50%)* [c]	1.4
		0.05 (50%)*	0.6
β55 Met→Ala	0.20 A	0.11 A	1.2
→Gly	0.21 A	0.11 A	1.2
β93 Cys→Ala	0.19 A	0.09 A	1.0
β95 Lys→Ala	0.14 A	0.08 A	0.9
β96 Leu→Ala	0.26 A	0.14 A	1.6
β97 His→Ala	0.33 (78%), 0.16 (22%)	0.11 A	1.2
β98 Val→Ala	0.3 (82%), 0.14 (18%)	0.10	1.1
β100 Pro→Ala	0.21 A	0.10 A	1.1
→Gly	0.33	0.14 A	1.6
β102 Asn→Ala	0.07 (>95%)	0.08 (50%)*	1.1
		0.03 (50%)*	0.3
β108 Asn→Ala	0.14 A	0.08 A	0.9
→Gly	0.14 A	0.07 A	0.8
β119 Gly→Ala	0.15 A	0.08 A	0.9
β124 Pro→Ala	4.4 (35%), 0.38 (65%)	5.5 (20%), 0.27 (80%)	61.1 3.0
β125 Pro→Ala	0.16 A	0.09 A	1.0
β145 Tyr→Ala	4.3 (45%) 1.1 A (55%)	0.34 A	3.8
→Ala XL99α	0.88 A	0.27 A	3.0
→Gly	4.6 (64%) 1.1 A (36%)	0.34 A	3.8
	β Chain Double Mutants		
β37 Trp→Ala, 108Asn→Ala	5.0 (19%), 0.9 (81%)	0.6 A	6.7
	α Chain Variants		
α1 Val→Met	0.17	0.09	
α40 Lys→Gly	2.5 (35%), 0.56 (65%)	0.16 A	1.8
α42 Tyr→Ala	8.3 (8%), 0.52 (92%)	0.16 A	1.8
→Ala XL99α	0.42 A		
α91 Leu→Ala	1.3 (50%)*	1.3 (50%)*	14.4
	0.35 (50%)*	0.08 (50%)*	0.9
α92 Arg→Ala	0.68 A	0.50 A	5.6
α94 Asp→Ala	0.27 A	0.17	1.9
→Gly	0.37 A	0.29 (50%)*	3.2
		0.15 (50%)*	1.7
α95 Pro→Ala	7.0 (15%), 0.3 (85%)	0.16 A	1.8
α95 Pro→Gly	0.31 A	0.16 A	1.8
α140 Tyr→Ala	7.0 (10%) 1.7 (90%)	heterogeneous 1.4−0.2	
→Gly	6.7 (55%) 2.3 (45%)	0.91 A	10.1

[a] The "A" indicates an autoaccelerating reaction. [b] This refers to the cross-linking of the two α chains between their lysine 99 ϵ amino groups by means of a fumarate bridge. [c] The asterisk indicates that in fitting these data the relative amounts of the two kinetic components were set as equal.

100 μM IHP. All mutant subunits actually contain the substitution of interest along with the replacement of the N-terminal valine by methionine. Therefore, to discern the functional effects of a given mutation, comparison should be made with the βV1M variant, in the case of β mutants, and with the αV1M variant, in the case of α mutants. However, within the error limits of our kinetic measurements, ±10%, the αV1M and βV1M substitutions have no effect on the kinetics of the reaction of CO with hemoglobin, permitting the use of HbA as the reference standard for this parameter. Data are also included for the cross-linked derivatives of three of the variants. An "A" following a rate constant indicates that the reaction is autocatalytic, i.e., accelerating with an apparent rate which increases as the reaction proceeds. In these cases, the rate constant quoted represents the best fit of the data to a single exponential function. For some mutants, the reaction observed is heterogeneous. Under these circumstances, the time course of the reaction was fitted to a sum of two exponentials, and all reaction rate constants are reported along with the percentage of the total reaction attributable to each kinetic process. In a few cases, in which there was reason to believe that two kinetic phases were the result of observing the separate kinetic processes for the two types of subunits, data were fitted to two exponential functions of equal magnitude to give a 50:50 fit. Such fits are denoted by an asterisk, and are only reported when they reproduce the data well.

The kinetics for the reaction of native human HbA with CO are accelerating with an overall rate constant of 0.18 μM^{-1} s^{-1}. The addition of 100 μM IHP reduces the rate of the reaction by roughly half to 0.09 μM^{-1} s^{-1}. As will be discussed, a number of the variants in Table 1 are significantly dissociated into $\alpha\beta$ dimers even when deoxygenated, and 100 μM IHP is very effective in reassembling such hemoglobins into tetramers.

For 17 of the variants examined, the effect of the deletion of the amino acid side chain, both in the presence and in the absence of IHP, is to merely alter the reaction rate constant for the single kinetic process. Twelve other mutants exhibit biphasic kinetics in the absence of IHP, while having homogeneous or accelerating kinetics in the presence of IHP. For 10 of these, at least 1 of the kinetic phases observed in the absence of IHP has a very large combination rate constant. As will be discussed in the next section, in these cases it is reasonable to hypothesize that in the absence of IHP there is significant dissociation of the deoxygenated protein into $\alpha\beta$ dimers which react rapidly with CO. Because of the strong preferential binding of IHP to the deoxygenated, T state tetramer, the presence of IHP shifts the dimer−tetramer equilibrium toward the tetramer to such an extent that the rapid kinetic phase becomes undetectable.

Along with the 29 mutants which bind CO with monophasic kinetics in the presence of IHP, there are 6 which remain or become biphasic in the presence of IHP. Three of these, βF42A, βN102A, and αD94G, have a single accelerating kinetic phase in the absence of IHP, but in its presence exhibit two kinetically distinguishable kinetic phases of equal magnitude. It is hypothesized that these two, equal kinetic phases represent the properties of the α and β chains within the low-affinity T state. This would require that the transition from the low-affinity T quaternary state to high-affinity forms of these variants be somehow inhibited or delayed.

There remain three variants with properties more complex than those described above. αL91A is biphasic under both experimental conditions, with the two phases having equal magnitudes within experimental error. The rate constant associated with the rapid phase is not large enough to be due to $\alpha\beta$ dimers, and is insensitive to IHP. The rate constant associated with the slower phase, on the other hand, is strongly affected by IHP. In the presence of IHP, the two rate constants differ by a factor of 16. It appears reasonable to hypothesize that this mutation has greatly increased the rate of CO binding to one type of subunit within the tetramer and rendered this subunit type insensitive to IHP. In the absence of IHP, the rate of CO binding with the second type of subunit has been increased less than 2-fold relative to HbA and still retains its IHP sensitivity. In the presence of 100 μM IHP, CO combines with these slowly reacting hemes at the same rate as with HbA. There is no doubt that the addition of 100 μM IHP results in a population of T state tetramers. As was previously shown for a number of β37 variants (*13*), the kinetic transition resulting from IHP addition does not require the IHP concentration be as great as 100 μM. The full effect of IHP addition to αL91A is achieved at an IHP concentration between 1 and 5 μM (data not shown). The only structure of Hb which can be saturated with IHP at such a low concentration is the T state. Since the side chain of αL91 lies in the vicinity of the heme of the α subunit, and not in the $\alpha1\beta2$ interface, it is suspected that the rapidly reacting subunit is the mutant α chain. βP124A exhibits two, unequal kinetic phases under both experimental conditions. The rate constants associated with the more rapid phases are consistent with the properties of $\alpha\beta$ dimers. However, one must wonder why IHP fails to achieve the full assembly of the deoxygenated dimers into deoxy, T state tetramers. It should be noted that this proline residue occurs at the bend between the G and H helices of the β chain. One can hypothesize that this proline residue is important for the proper orientation of the H helix. At the end of the H helix, one finds the C terminus of the β chains, which furnishes essential interactions for the proper binding of IHP. It may be that the replacement of this proline results in a misorientation of the H helix and disrupts the IHP binding site, with the resultant loss of the strong, preferential binding of IHP to the deoxygenated hemoglobin tetramer. In support of a significant disruption of overall structure is the finding that among all of the mutants, this is the only one that fails to crystallize under the conditions normally used to crystallize deoxyHbA. The remaining variant defies a simple explanation. αY140A is heterogeneous in the presence of IHP; i.e., it cannot be fitted by two kinetic phases nor uniquely fitted by three. Under these same conditions, αY140G is kinetically homogeneous. Although it is not possible to exclude an artifact in the preparation of the αY140A variant, two totally independent preparations were made, starting with different batches of bacterial cells. Both preparations, which yielded single peaks in HPLC and single bands on gel electrophoresis, displayed kinetic heterogeneity in the presence of IHP. The procedure for these preparations was the same as that which yields the homogeneous preparations of the βY140G variant. The possibility always exists that a variant might fold into more than one functionally distinguishable conformer. If these conformers reequilibrate with one another with a relaxation time which is long compared to the time constant for CO binding, then kinetic heterogeneity will be observed.

Reasons for the Assignment of Rapid Phases in CO Combination Kinetics to $\alpha\beta$ Dimers. The foundations for this hypothesis lie in the thermodynamic analyses of Ackers and co-workers (*2*) and in the analysis of the origins of the kinetics of CO recombination following flash photolysis by Edelstein et al. (*3*). Ackers et al. (*2*) have carefully analyzed the thermodynamic linkage between ligand binding and the free energy of assembly of $\alpha\beta$ dimers into Hb tetramers. Because of the large difference in the ligand affinities of the dimers and Hb tetramers, the assembly free energy changes substantially with the attachment of ligands at the heme groups. For deoxygenated HbA, the assembly is energetic enough that $\alpha\beta$ dimers are almost undetectable. However, for fully liganded HbA, the stability of the tetramer is so reduced that at the concentration used in the kinetic experiments reported here roughly 60% of the tetramers are dissociated into $\alpha\beta$ dimers. One result of this dissociation is the pronounced concentration dependence of the apparent oxygen affinity of hemoglobin in solution (*25*). The oxygen affinity of the Hb tetramer can be accurately determined only by measurement of the concentration dependence of apparent affinity and appropriate extrapolation.

In measuring CO recombination, one begins with CO-saturated Hb at a known CO concentration and photolyzes the CO off the protein using a light pulse of sufficient duration to pump all of the ligand out of the protein matrix despite geminate rebinding. One then follows the second-order recombination of CO with the unliganded Hb, the tetramer of which has switched to the T quaternary state at a rate much greater than that at which CO binds (*3*, *13*). CO recombination differs from CO combination with deoxyHb in that the relative amounts of $\alpha\beta$ dimers and Hb tetramers in solution should be those appropriate for a solution of liganded Hb as dimer assembly is slow with respect to the rate of CO combination at 20 μM CO. One observes a two-phase kinetic process, the slow phase having the rate expected for deoxygenated Hb tetramer and the fast phase having a rate consistent with the R state of Hb, isolated chains of Hb, or $\alpha\beta$ dimers. Using a combination of sedimentation equilibrium analysis and measurements of CO recombination at different Hb concentrations, Edelstein et al. (*3*) conclusively demonstrated that the rapid kinetic process corresponds to the recombination of CO with $\alpha\beta$ dimers. Cross-linking the Hb molecule between its two α99 Lys residues has been shown to eliminate the rapid kinetic phase (*13*).

The first mutants for which a rapid kinetic phase was observed in the reaction of CO with deoxygenated Hb following rapid mixing were substitutions of the β37 Trp residue. Because of the similarity with the kinetic pattern seen in CO recombination reactions, it was postulated that these variant tetramers were so destabilized as to be significantly dissociated into $\alpha\beta$ dimers, even when fully deoxygenated (*13*). This was subsequently shown to be the case for βW37G and βW37E by direct measurement (*26*). The presence of IHP eliminates the rapid kinetic phase in CO combination whereas it fails to do so in CO recombination kinetics. IHP exhibits strong, specific binding to the T quaternary state of the Hb tetramer, shifting the equilibrium of deoxyHb toward the intact tetramer and leaving too few

dimers to easily detect. In a solution of ligand-saturated Hb, there are essentially only R state tetramers to which IHP binds only weakly, thereby causing only small changes in the dimer−tetramer equilibrium. Again, as shown in Table 1, cross-linking the Hb tetramers of αY42A, *β*W37G, and *β*Y145A eliminates the rapid phase.

It is not possible to say with certainty that the above is the appropriate or only explanation for all of the rapid phases observed in the CO combination kinetics reported in Table 1. An alternative possibility to be considered is the presence of multiple conformers of the Hb tetramers in solution following photolysis, which for some reason reequilibrate with one another slowly. Preferential IHP binding might eliminate the rapid kinetic phase in this scenario, but its complete elimination as well by cross-linking the α*β* dimers within the tetramer seems a remarkable coincidence. For the moment, it seems most reasonable to suppose that the rapid phases in both CO combination and CO recombination have the same origin.

Distribution of the Effects of Deletion of the Side Chains of Individual Residues. For the most part, the presence of IHP eliminates dissociation of unstable mutant tetramers into α*β* dimers. Therefore, it is in the presence of this allosteric effector that the rate constants for CO combination best reflect the properties of the fully assembled, deoxygenated tetramer. Furthermore, it has been found that the kinetics of CO combination in the presence of IHP correlate well with the oxygen affinities of the crystalline T states of chemically modified and variant hemoglobins (*22*, *27*, *28*). Therefore, to estimate the magnitudes of the effects of mutations on the properties of the deoxygenated T state tetramer, kinetic properties in the presence of IHP were compared. The fourth column of Table 1 lists the "effect ratio", the ratio of the rate constant for CO combination with the variant to the rate constant for CO combination with HbA in the presence of IHP. In Figure 1 the locations of the α carbons of the mutant amino acids within the Hb molecule are indicated, and these are color-coded, based on the effect ratio, to indicate the magnitude and direction of the effects of each mutation on the kinetics of CO combination with the deoxygenated Hb tetramer in the presence of IHP. Purple indicates a ratio less than 0.7, light blue between 0.7 and 1.5, green between 1.6 and 2.5, orange between 2.6 and 5.0, and red greater than 5.0. In the majority of cases, the colors in this figure are chosen for the Ala substitutions. The exceptions are α140, α40, and *β*34 which are Gly substitutions. For the latter two sequence positions, we have not produced the Ala substitutions. For the α140 position, the Ala substitution is so kinetically heterogeneous that it is unclear how to represent it. Other exceptions are *β*146 and α141, which represent deletions of the C-terminal residues, i.e., desHis146*β* and desArg141α (*28*). Finally α1 and *β*1 indicate the effects of the Val → Met substitution which is found on all of the mutant chains. Circles indicate variants which are kinetically homogeneous in the presence of IHP. Squares, all of which have two colors, indicate variants with biphasic kinetics. Surprisingly, the distribution within the protein of mutational effects on the properties of the deoxygenated T state is in no way uniform. All but one of the mutations which result in large increases in the rate of CO combination with the deoxygenated T state (red and orange) are located in the region of the α1*β*2 interface between the FG corner and

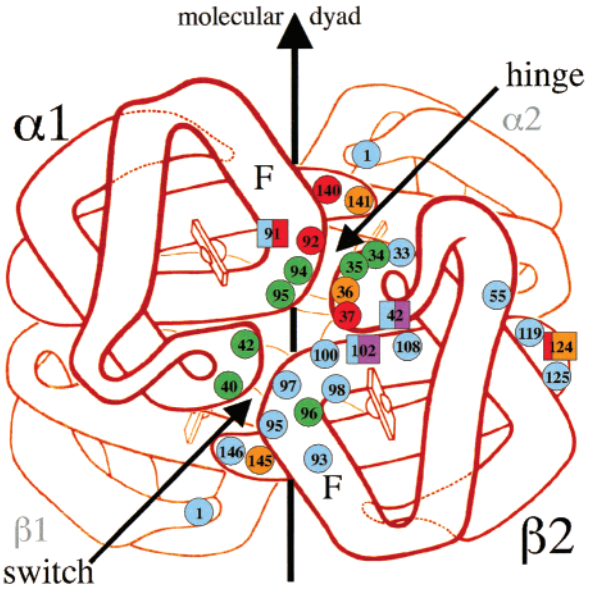

FIGURE 1: Distribution of effects of Ala or Gly substitutions within the HbA molecule on the rate constant for the combination of CO with the deoxygenated Hb molecule. Using one of the Irving Geis diagrams of the hemoglobin molecule, from Dickerson and Geis (*29*), the positions of the α carbons of the residues which have been examined are indicated. At each residue, the magnitude of the effect of essentially deleting the normal amino acid side chain is indicated by color. Purple indicates a ratio of the rate constant of the mutant to that of HbA less that 0.7, light blue between 0.7 and 1.5, green between 1.6 and 2.5, orange between 2.6 and 5.0, and red greater than 5.0. Square symbols with two colors designate biphasic kinetic processes and indicate the two rate constants. Further details are described in the text. Note: The rights to the illustration by Irving Geis are owned by Howard Hughes Medical Institute. It is not to be used without permission.

C-terminal regions of the α chains and the C helix of the *β* chains, i.e., the hinge region.

*β*Y145 is the only residue located in the vicinity of the switch region of the α1*β*2 interface whose mutation has a substantial kinetic effect. It is interesting to compare the effects of mutations at this residue to the effects of mutations at the analogous residue of the α chains, α140 tyrosine. In the T quaternary structure of HbA, the two penultimate tyrosine residues are to a first approximation symmetrically arranged, with the phenolic hydroxyl of α140 H-bonded to the carbonyl group of α93 of the same α subunit and that of *β*145 H-bonded to the analogous carbonyl group of *β*98, again residue FG5 of the same subunit. Both of these residues undergo major conformational transitions in the course of ligand binding and appear to have central roles in the normal functioning of Hb. In any case, the contributions of these two residues to the properties of the deoxygenated T state are decidedly dissimilar. The αY140G variant reacts with CO 10-fold more rapidly than does HbA, while the effect of replacing *β*Y145 with either Gly or Ala is less than a 4-fold increase in CO combination rate. The phenylalanyl substitutions of αY140 and *β*Y145 have also been prepared and their CO combination kinetics examined. For the *β*145 residue, the substitution of phenylalanine for tyrosine has no significant effect on CO combination kinetics in either the absence or the presence of IHP. On the other hand, for the α140 residue, this same substitution increases the rate of CO combination in both the presence and absence of IHP

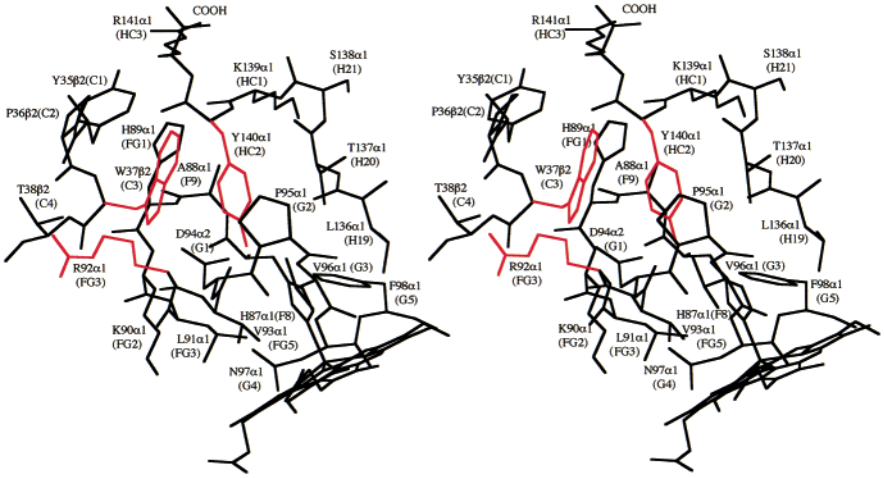

FIGURE 2: This figure is from ref (*31*) and is used with permission of the authors. It shows the three-dimensional structure of a portion of the hinge region of the α1*β*2 interface and includes all five of the residues whose mutation to Ala or Gly results in large increases in the rate of CO combination (residues which are red or orange in Figure 1). The three most effective residues, αY140, *β*W37, and αR92, which are red in Figure 1, are highlighted here in red for clarity. The other two, *β*P36 and αR141, are also shown.

by somewhat over 5-fold. These differences in the sensitivity of the properties of the deoxygenated T state of Hb to the status of these two tyrosines may well lie in the differences in their direct involvement with the α1*β*2 interface. In deoxyHb, the side chain of αY140 tyrosine is in strong, close (3.5 Å) van der Waals contact with the side chain of *β*W37 and in weaker contact (3.8 Å) with *β*P36, both across the α1*β*2 interface. The *β*145 tyrosine has only a single very weak contact (3.8 Å) across the α1*β*2 interface with αT41.

A direct correlation between the mobility of the C-terminal residues of the α subunits within deoxyHb crystals and the rate of CO combination with the deoxyHb in solution has been observed for *β*W37 variants (*13*, *22*, *26*, *27*, *30*, *31*), for desArgHb (*32*), and for *β*Y35A (*33*). It seems clear that the mobility of the α subunit C terminus will depend in large part on the mobility of the αY140 side chain. That mobility appears to be most directly limited by the strong interaction of αY140 with *β*W37. The adjacent residues with substantial effects on CO combination, *β*P36, αR92, and αR141, may alter α140 mobility by direct interaction as in the case of *β*P36, by affecting the mobility of the α subunit C terminus generally as with desArg, or by affecting the mobility of *β*W37 through direct interaction as could be the case for αR92. The structure of the hinge region of the α1*β*2 interface containing these five key residues is shown in Figure 2. The three residues with the greatest effect on CO combination kinetics (red in Figure 1) are highlighted in red. However, both *β*P36 and αR141 are also clearly visible.

CO Combination with FeZn Hybrids of Hb Variants. It was suspected that within the region of the α1*β*2 interface mutational effects on the functional properties of the deoxygenated T state might fall into two classes. The most obvious are the local effects where a mutation within a particular subunit alters the properties of the heme group of that subunit. As previously discussed, αL91A is probably an example of a mutation producing such a local effect. The mutation results in two rapidly reacting heme groups which have lost their normal sensitivity to the presence of IHP. Following the reaction of the first two hemes, the second two hemes bind CO at a rate which, in the presence of IHP, is indistinguishable from the rate at which CO reacts with HbA. In the absence of IHP, the slower kinetic phase seen for the mutant is some 2-fold more rapid than the rate at which CO binds HbA. This may reflect residual cooperativity between the binding of ligand to the two types of subunits in the absence of the organic phosphate. On the other hand, previous results of studies of *β*W37 variants (*13*, *26*) and the equilibrium and kinetic results presented here for the αY140 variants are consistent with all four hemes being of high affinity within the deoxygenated tetramer. However, these results are not conclusive, as they might be obtained from cooperativity superimposed on significant subunit heterogeneity within the T state. Ligand binding to a pair of high-affinity subunits might increase the ligand affinities of the remaining subunit hemes to give apparently homogeneous kinetics and high overall oxygen affinity.

To directly assess the effects of a mutation on the two different chain types within the deoxygenated hemoglobin tetramer, symmetrical FeZn hybrids were used. In these hybrids, the hemes of either the α or the *β* chains were replaced with Zn protoporphyrin IX. Zn porphyrin in hemoglobin cannot bind ligand, and instead remains permanently unliganded. The careful thermodynamic measurements of Ackers et al. (*2*) demonstrate that Zn porphyrin is an excellent mimic of deoxygenated heme. If the rates of CO combination with these hybrids are measured, the rate constants observed are attributable to the heme containing chains alone. Because of the photosensitivity of Zn porphyrin, all kinetic measurements on FeZn hybrids were carried out in very dim light. However, this photosensitivity is not so great as to result in measurable changes as a result of exposure to the monochromatic light beam in the stopped-flow apparatus.

The kinetics of the reactions of CO with the FeZn hybrids of HbA, *β*W37E, cross-linked *β*W37E, *β*W37A, αY140G, αY140A, and *β*Y145G are reported in Table 2. The choice of *β*W37E rather than *β*W37A or -G for cross-linking was based entirely on the availability of sufficient material with which to prepare the samples. Most of the results are reported as k_1 and k_2 from eq 1 (see Experimental Procedures). However, as expected from the data in Table 1, in the absence of IHP all of the un-cross-linked mutants in Table

Table 2: CO Combination Kinetics of Fe−Zn Hybrids[a]

	no IHP		+IHP	
	k_1	k_2	k_1	k_2
α[Fe]β[Zn]	0.13	0.10	0.10	0.10
α[Zn]β[Fe]	0.11	0.09	0.046	0.036
α[Fe]β_{W37E}[Zn]	*[5.7 (53%), 3.1 (47%)]*		1.2	1.0
α[Zn]β_{W37E}[Fe]	*[4.0 (50%), 1.7 (50%)]*		1.2	0.85
αXL[Fe]β_{W37E}[Zn]	1.0	1.1	1.0	1.1
αXL[Zn]β_{W37E}[Fe]	1.6	1.1	1.05	0.72
α[Fe]β_{W37A}[Zn]	*[4.6 (50%), 0.66 (50%)]*		0.49	0.60
α[Zn]β_{W37A}[Fe]	*[2.8 (50%), 0.75 (50%)]*		0.42	0.35
α_{Y140G}[Fe]β[Zn]	*[7.3 (76%), 1.9 (24%)]*		1.5	1.4
α_{Y140G}[Zn]β[Fe]	*[4.8 (79%), 0.64 (21%)]*		0.18	0.16
α_{Y140A}[Fe]β[Zn]	*[8.1 (44%), 1.6 (56%)]*		1.2	1.0
α_{Y140A}[Zn]β[Fe]	*[3.7 (36%), 0.42 (64%)]*		0.09	0.07
α[Fe]β_{Y145G}[Zn]	*[4.2 (52%), 0.26 (48%)]*		0.13	0.10
α[Zn]β_{Y145G}[Fe]	*[6.3 (62%), 0.98 (38%)]*		0.40	0.24

[a] Second-order rate constants for a 2-step sequential mechanism or *[for a sum of two exponential functions]* (μM^{-1} s^{-1}).

2 appear to be significantly dissociated into αβ dimer when unliganded, rendering eq 1 invalid. As already discussed, it was previously shown (*13*, *26*) that in the absence of IHP most β37 variants, particularly βW37A, βW37G, and βW37E, exhibited considerable dissociation into αβ dimers at the Hb concentration used for CO combination measurements, 2 μM in heme, even when deoxygenated. One indication of this dissociation was a very large effect of cross-linking on the kinetics of CO combination in the absence of IHP. For βW37G, this effect is seen in Table 1 where cross-linking this variant is shown to significantly reduce the initial rate of the reaction with CO and change the reaction from a kinetically biphasic to a homogeneous one. A similar effect of cross-linking βY145A is also shown in Table 1. With the FeZn hybrids of βW37E, it is found that cross-linking reduced the initial rate of CO binding to the α subunits by 5-fold and the rate of binding to the β subunits by 2-fold. The reactions of the FeZn hybrids of βW37A and βY145G in the absence of IHP are very heterogeneous and cannot be fitted to eq 1. Therefore, it appears reasonable to conclude that the deoxygenated FeZn hybrids of βW37E, βW37A, and βY145G are dissociated significantly into αβ dimers in the absence of IHP. There is no direct proof that in the absence of IHP deoxygenated αY140G and αY140A are dissociated into dimers. The properties of the deoxygenated tetramers of these two variants under these conditions are not known. However, CO combination with the FeZn hybrids of these variants can be fitted to a two-step, sequential mechanism only when IHP is present. Therefore, the data obtained for the un-cross-linked mutants in the absence of IHP are fitted to a sum of two exponential functions, and the two rate constants and percent contributions of each kinetic component to the reaction are reported. The latter results appear in italics in Table 2.

As can be seen in Table 2, the βW37E substitution increases the rate constants for CO combination with both the α and β subunits within the deoxygenated tetramer, by 12-fold for the α subunits and by 26-fold for the β subunits. It should be noted that to evaluate the kinetic properties of the deoxygenated Hb tetramer, the relevant rate constant is k_1. The properties of cross-linked βW37E permit the observation of the effect of IHP on the properties of the individual subunits within the deoxygenated T state of this variant. In this regard, IHP is found to have no effect on the rate of CO binding to the α subunits while decreasing the rate of binding to the β subunits by 34%. The kinetic results obtained with FeZn hybrids of HbA also exhibit a greater effect of IHP on the rate of CO binding to β subunits than to the α subunits. The βW37A substitution has smaller kinetic effects than the βW37E substitution, increasing the rate constant for CO combination to the α subunits by 5-fold and that for the β subunits by 9-fold. The two Fe−Zn hybrids of αY140G are more dissimilar than those of the β37 variants. Within the deoxygenated T state, the αY140G mutation perturbs the α subunits significantly more than the β subunits. The rate constant for the combination of CO with the α subunits is increased 15-fold while that for the β subunits is increased 4-fold. The difference between the effects of the αY140A mutation on the α and β subunits within the deoxygenated T state is greater still, with a 12-fold increase in the rate constant for CO binding to the α subunit and a 2-fold increase in the same rate constant for the β subunit. Mutations at both β37 and α140 have global effects, altering the properties of the neighboring partner subunits as well as those of the subunits in which they are located. The βY145G substitution has strikingly little effect on the properties of the α subunits within the T state. In fact, the close correspondence between the kinetic properties of the α chains of the variant and those of HbA can be used as evidence that IHP addition yields the low-affinity T state of this variant. On the other hand, this mutation appears to increase the rate of CO binding to the β subunit within the deoxygenated T state by more than 8-fold. The latter fit is imperfect, suggesting heterogeneity in the sample. However, there was no indication of a significant number of more slowly reacting heme groups. Furthermore, this mutation increases the overall rate of CO binding to the deoxygenated protein containing heme groups on all four subunits by almost 4-fold, which, given the lack of a significant effect on the kinetics of binding to the α subunits, requires a substantial effect on the β subunits.

Equilibrium of Oxygen Binding to Crystalline T Structures. A second effective way of characterizing the functional properties of the low-affinity T quaternary state of hemoglobin variants is measurement of the oxygen affinity of the crystalline T state (*24*). This measurement has been carried out for four of the variants in Table 1, βN108G, βN102A, βY35A, and αY42A, as well as for βW37E. Two of the parameters determined are the *p*50, the partial pressure of oxygen required for half-saturation, and the Hill coefficient, *n*. These are shown in Table 3. T state crystals of βW37E pose a special experimental problem. Crystals of such high oxygen affinity tax the procedures for carrying out these equilibrium measurements. It is a general observation that the equilibration time increases with increasing affinity, presumably as a result of the reduced concentration of free oxygen diffusing through the crystal. For the present study, it was found that the time required for equilibration of βW37E crystals varied from 20 to 28 h. This results in the formation of considerable methemoglobin, always at least 30%, and even greater amounts at low saturations. However, fractional saturation of the ferrous heme groups appeared to be independent of the percent methemoglobin. Still the data obtained are of much lower quality than those contained in previous reports of lower affinity crystals (*22*, *24*, *28*). As

Table 3: Equilibria of Oxygen Binding to Crystals of Deoxyhemoglobin

variant	*p*50 (Torr)	*n* (Hill)[a]
HbA[b]	135	1.0
βN108G	125	0.93
βN102A	112	0.94
βY35A[c]	80	1.15
βW37E	2.6	see[d]
αY42A	33	1.06

[a] There is no distinction between *n* and n_{max} for oxygen binding to Hb crystals since their Hill coefficients do not vary systematically with fractional saturation. [b] Reference (*34*). [c] Kavanaugh et al. (*33*) have found that crystals of βY35A are unstable above 50% saturation with oxygen, undergoing an irreversible transitions to higher affinity. For this reason, data for only the first half of the saturation curve are available. [d] The Hill coefficient of this variant is poorly defined (see text).

shown in Table 3 the *p*50 appears to be 2.6 Torr. However, the data indicate a Hill coefficient well above unity. Given the difficulty of these measurements and the possibility of nonrandom errors, the significance of the apparent cooperativity is uncertain.

If one compares the values of *p*50 of the crystals with the rate constants for the combination of CO with the four variants in the presence of IHP (Table 1), a clear inverse correlation is observed. This supports the proposition that the kinetic parameter is a good indicator of the ligand affinity of the deoxygenated or low-affinity T quaternary state of each variant. The conclusion that the βW37E mutation increases the ligand affinity of both the α and β subunits within the deoxygenated T state is supported by the high oxygen affinity of the T state crystals of this variant and the fact that exposure of these crystals to air at 15 °C results in essentially complete saturation with oxygen. Crystals of HbA are approximately half-saturated with oxygen under the same conditions. Since the crystalline T state of hemoglobin A appears to be constrained in the low-affinity T state structure with little or no cooperativity, no sensitivity to pH or polyanions, and an oxygen affinity similar to that of the first step of oxygen binding to HbA in solution in the presence of IHP (*24*, *34*), the presence of only high-affinity heme groups in βW37E crystals again indicates that the mutation affects both the α and β subunits within the deoxygenated T state tetramer.

The sensitivity of both the α and β subunits to the state of the β37 residue can also be inferred from earlier studies of the equilibria of oxygen binding to the crystalline T state of Hb Rothschild, βW37R, by Rivetti et al. (*22*). It was found that chloride ion decreased the oxygen affinity of both types of subunits within the crystal and at the same time induced cooperativity in oxygen binding. The cooperativity appeared to result from simultaneous negative allosteric linkage between chloride binding to the β37 arginine and the binding of oxygen to both the α and β hemes.

Equilibria of Oxygen Binding in Solution. For the majority of the variants, the overall effect of the mutation on functional properties has been assessed by measurement of equilibria of oxygen binding in solution, and the results are presented in Table 4. Again, *p*50, the partial pressure of oxygen required for half-saturation, and the maximum Hill coefficient, *n*, are reported. All equilibrium measurements were carried out at pH 7 in the absence of IHP. Again, the properties of normal human HbA and the βV1M and αV1M variants are included for comparison. Although the βV1M substitution has no effect on CO combination kinetics, it is known from the results of Doyle et al. (*6*) that it lowers overall oxygen affinity somewhat. The data in Table 4 are in agreement with this earlier report. In contrast, the αV1M substitution is reported by Hui et al. (*10*) to be without significant effect on the equilibrium properties of hemoglobin. Given an estimated error of $\pm$10% for the data in this Table 4, the difference observed between the oxygen affinity of HbA and αV1M is again not significant.

Table 4: Equilibrium of O_2 Binding in Solution to Ala and Gly Substitutions (20 °C, 0.1 M HCl-bisTris Buffer, pH 7)

	O_2 equilibria parameters		
variant	$p50(O_2)$	n_{max} (Hill)[a]	effect ratio
HbA	4.6	2.8	
β1 Val→Met	6.7	2.8	1.5 (vs HbA)
β33 Val→Ala	7.3	2.4	0.92
β34 Val→Gly	2.3	2.6	2.9
β35 Tyr→Ala	1.7	2.7	3.9
β36 Pro→Ala	1.7	2.5	3.9
β37 Trp→Ala[b]	2.2	1.4	3.0
→Gly[b]	1.6	1.2	4.2
β42 Phe→Ala	9.6	0.86	0.70
β55 Met→Ala	4.8	2.5	1.4
→Gly	4.6	2.1	1.5
β93 Cys→Ala	6.5	2.7	1.0
β95 Lys→Ala	8.8	2.8	0.76
β96 Leu→Ala	4.9	1.6	1.4
β97 His→Ala	1.6	3.2	4.2
β100 Pro→Ala	2.2	2.1	3.0
→Gly	0.9	2.3	7.4
β102 Asn→Ala	26.3	1.6	0.25
β108 Asn→Gly	13.2	2.3	0.51
β119 Gly→Ala	8.1	2.2	0.83
β125 Pro→Ala	7.3	2.3	0.92
β145 Tyr→Ala	0.3	1.6	22
β145 Tyr→Ala, αXL99α[c]	0.76	1.6	8.8
β146 His→0[d]	1.1	2.0	4.2
α1 Val→Met	5.0	2.8	1.1 (vs HbA)
α40 Lys→Gly	0.68	1.7	7.4
α42 Tyr→Ala	1.8	1.9	2.8
α91 Leu→Ala	7.1	1.2	0.70
α94 Asp→Gly	7.9	1.3	0.63
α140 Tyr→Gly	0.35	1.2	14.3
α141 Arg→0[e]	0.55	1.6	8.4

[a] In general, the Hill plots of these data are asymmetrical with the maximum Hill coefficient occurring in the second half of the saturation process. This is similar to the findings of Doyle et al. (*6*) for the βV1M construct. [b] From Kiger et al. (*26*). These measurements were carried out at 21.5 °C at hemoglobin concentrations of 635 μM (heme) for βW37A and 675 μM for βW37G. [c] For this measurement, the hemoglobin concentration was 25 μM. [d] This is desHis-hemoglobin, HbA from which the β146 histidine residues have been enzymatically removed (*28*). [e] This is desArg-hemoglobin, HbA from which the α141 arginine residues have been enzymatically removed (*32*).

As in Table 1, the final column of Table 4 lists the "effect ratio" for each variant. For β chain variants, this is the ratio of the *p*50 for βV1M to the *p*50 of the variant, and for α chain variants, it is the ratio of the *p*50 of αV1M to that of the variant. In Figure 3 the locations of these mutations within the Hb molecule are indicated, and again each mutation is color-coded according to its effect ratio. As in Figure 1, purple indicates a ratio less than 0.7, light blue between 0.7 and 1.5, green between 1.6 and 2.5, orange between 2.6 and 5.0, and red greater than 5.0. The colors represent primarily the properties of Ala substitutions. The

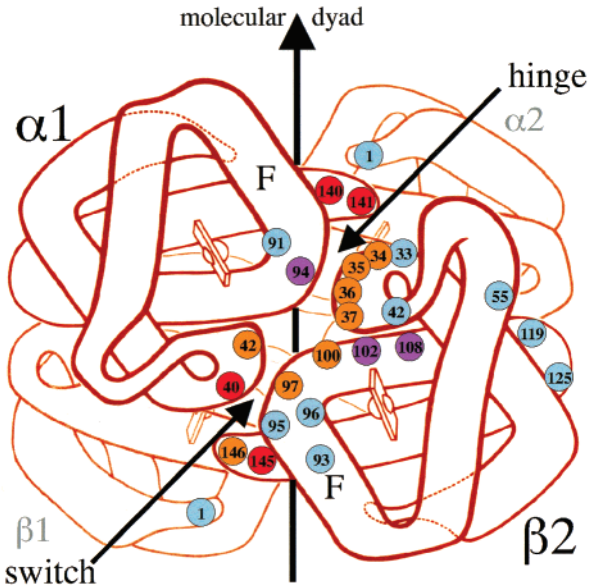

FIGURE 3: Distribution of effects of Ala or Gly substitutions within the HbA molecule on the $p50(O_2)$, the partial pressure of oxygen required for half-saturation. Using the same diagram by Irving Geis as in Figure 1, the positions of the α carbons of the residues examined in this way are indicated. At each sequence position, the magnitude of the effect of deleting the normal amino acid side chain in indicated by color. As in Figure 1, purple indicates a ratio of the *p*50 of the mutant to that of the reference structure of less than 0.7, light blue between 0.7 and 1.5, green between 1.6 and 2.5, orange between 2.6 and 5.0, and red greater than 5.0. Further details are in the text. Note: The rights to the illustration by Irving Geis are owned by Howard Hughes Medical Institute. It is not to be used without permission.

exceptions are α140, α40, *β*34, and α94, which are Gly substitutions, and α1 and *β*1, which indicate the effects of the Val → Met substitutions at the N-termini.

If Tables 1 and 4 are compared, it is evident that there is not a close correlation between the CO combination rate constants and the overall oxygen affinities of the variants. Given the variety of parameters which can affect oxygen affinity, this lack of correlation is not unexpected. One of these parameters is clearly the ligand affinity of the deoxygenated tetramer in the T quaternary state, as predicted by the rate of CO binding to the deoxygenated Hb molecules in the presence of IHP. However, oxygen affinity is also affected by the nature and sequence of affinity changes which accompany the stepwise saturation of the tetrameric protein with oxygen. This would include functional changes within the T quaternary state as described by Ackers et al. (*2*) and the point during the saturation process at which transition to the high-affinity R quaternary structure occurs. All but one of the variants which exhibit homogeneous or accelerating CO combination kinetics in both the absence and presence of IHP also bind oxygen with Hill coefficients greater than 2. The exception is *β*L96A with an *n* value of 1.6. The *β*F42A, *β*N102A, αL91A, and αD94G variants exhibit two equal, relatively slow kinetic processes when CO combines in the presence of IHP. It has been suggested that the two phases represent the two types of subunits, and their appearance indicates that the transition from the T to R quaternary state may be inhibited. Consistent with this suggestion, all of these variants exhibit lower oxygen affinities than HbA and below average Hill coefficients. Finally, tetramer instability with respect to dissociation into α*β* dimers is also an important parameter. The *β*Y145A and αY140G variants have similar oxygen affinities, the two highest affinities we have measured for this set of Hb variants. However, their kinetic effect ratios are very different. It appears that in the absence of IHP these variants are extensively dissociated into α*β* dimers whose high affinities influence the apparent oxygen affinities. Cross-linking the *β*Y145A variant reduces its affinity by 2.5-fold.

As was found for the rate constants for CO combination, the largest increases in oxygen affinity result from mutations of residues in the vicinity of the α1*β*2 interface. However, it can be easily seen that there is not a close correspondence between the distributions of mutations which have large effects on CO binding kinetics and those which have large effects on oxygen affinity in solution. The mutations resulting in the largest increases in oxygen affinity (red and orange) are distributed roughly equally between the hinge and switch regions of the α1*β*2 interface. Although the hinge region of the α1*β*2 interface is of special significance to the properties of the low-affinity T quaternary state, mutations with substantial effects on the other parameters affecting overall ligand affinity are more widely scattered.

CONCLUSIONS

The hinge region of the α1*β*2 interface of the hemoglobin molecule exercises control over the ligand affinities of the hemes of all of the subunits within the hemoglobin tetramer. Mutations at *β*W37 and αY140 result in the largest increases in the rate of CO binding to the deoxygenated T quaternary state of hemoglobin observed among the mutations examined here. The side chains of these two residues are in close contact with one another across the α1*β*2 interface. Modifications at any of three adjacent residues, deletion of the side chain of αR92 or *β*P36 or complete deletion of αR141, result in smaller but still substantial increases in CO combination. It is hypothesized that it is the interaction between *β*W37 and αY140 which is the keystone for the interactions that result in the low ligand affinity of all four hemes in the deoxygenated T state of HbA. Deletion of the side chain of either residue, or even perturbation of the orientation or orientational stability of either by alteration of neighboring residues, profoundly affects all of the heme groups within the T state. Although mutations at other residues, such as αL91 and *β*Y145, can have profound local effects on the subunit in which they occur, the global influence of the *β*37−α140 contact appears to be unique.

ACKNOWLEDGMENT

We thank Dr. Jeffrey Kavanaugh, Dr. Arthur Arnone, and Ben Davis (University of Iowa), Program Project Group collaborators, for preparation of mutant globin genes and expression of them in *E. coli*, for preparation of the figures in this article, and for their many valuable ideas and suggestions throughout this work. We also thank Ellen Karasik for carrying out some of the oxygen equilibrium measurements.

REFERENCES

1. Brunori, M., Noble, R. W., Antonini, E., and Wyman, J. (1966) *J. Biol. Chem. 241*, 5238−5243.

2. Ackers, G. K., Holt, J. M., Huang, Y., Grinkova, Y., Klinger, A. L., and Denisov, I. (2000) *Proteins: Struct., Funct., Genet. Suppl 4*, 23−43.
3. Edelstein, S. J., Rehmar, M. J., Olson, J. S., and Gibson, Q. H. (1970) *J. Biol. Chem. 245*, 4372−4381.
4. Mueser, T. C., Rogers, P. H., and Arnone, A. (2000) *Biochemistry 39*, 15353−15364.
5. Riggs, A. F. (1981) *Methods Enzymol. 76*, 5−29.
6. Doyle, M. L., Lew, G., De Young, A., Kwiatkowski, L., Wierzba, A., Noble, R. W., and Ackers, G. K. (1992) *Biochemistry 31*, 8629−8639.
7. Bucci, E., and Fronticelli, C. (1965) *J. Biol. Chem. 240*, 551−552.
8. Hernan, R. A., Hui, H. L., Andracki, M. E., Noble, R. W., Sligar, S. G., Walder, J. A., and Walder, R. Y. (1992) *Biochemistry 31*, 8619−8628.
9. Hernan, R. A., and Sligar, S. G. (1995) *J. Biol. Chem. 270*, 26257−26264.
10. Hui, H. L., Kavanaugh, J. S., Doyle, M. L., Wierzba, A., Rogers, P. H., Arnone, A., Holt, J. M., Ackers, G. K., and Noble, R. W. (1999) *Biochemistry 38*, 1040−1049.
11. Chatterjee, R., Welty, E. V., Walder, R. Y., Pruitt, S. L., Rogers, P. H., Arnone, A., and Walder, J. A. (1986) *J. Biol. Chem. 261*, 9929−9937.
12. Snyder, S. R., Welty, E. V., Walder, R. Y., Williams, L. A., and Walder, J. A. (1987) *Proc. Natl. Acad. Sci. U.S.A. 84*, 7280−7284.
13. Kwiatkowski, L. D., Hui, H. L., Wierzba, A., Noble, R. W., Walder, R. Y., Peterson, E. S., Sligar, S. G., and Sanders, K. E. (1998) *Biochemistry 37*, 4325−4335.
14. Rossi-Fanelli, A., Antonini, E., and Caputo, A. (1958) *Biochim. Biophys. Acta 30*, 608.
15. Clegg, J. B., Naughton, M. A., and Weatherall, D. J. (1966) *J. Mol. Biol. 19*, 91−108.
16. Gibson, Q. H. (1959) *Biochem. J. 71*, 293.
17. Gibson, Q. H. (1959) *Prog. Biophys. Biophys. Chem. 9*, 1−50.
18. Nagel, R. L., Wittenberg, J. B., and Ranney, H. M. (1965) *Biochim. Biophys. Acta 100*, 286−289.
19. Allen, D. W., Guthe, K. F., and Wyman, J. (1950) *J. Biol. Chem. 187*, 393−410.
20. Hayashi, A., Suzuki, T., and Shin, M. (1973) *Biochim. Biophys. Acta 310*, 310−316.
21. Noble, R. W., DeYoung, A., Vitale, S., Cerdonio, M., and DiIorio, E. E. (1989) *Biochemistry 28*, 5288−5292.
22. Rivetti, C., Mozzarelli, A., Rossi, G. L., Kwiatkowski, L. D., Wierzba, A. M., and Noble, R. W. (1993) *Biochemistry 32*, 6411−6418.
23. Dvorak, J. A., and Stotler, W. F. (1971) *Exp. Cell Res. 68*, 144−148.
24. Rivetti, C., Mozzarelli, A., Rossi, G. L., Henry, E. R., and Eaton, W. A. (1993) *Biochemistry 32*, 2888−2906.
25. Ackers, G. K. (1998) *Adv. Protein Chem. 51*, 185−253.
26. Kiger, L., Klinger, A. L., Kwiatkowski, L. D., De Young, A., Doyle, M. L., Holt, J. M., Noble, R. W., and Ackers, G. K. (1998) *Biochemistry 37*, 4336−4345.
27. Kelly, R. M., Hui, H. L., and Noble, R. W. (1994) *Biochemistry 33*, 4363−4367.
28. Bettati, S., Kwiatkowski, L. D., Kavanaugh, J. S., Mozzarelli, A., Arnone, A., Rossi, Gi. L., and Noble, R. W. (1997) *J. Biol. Chem. 272*, 33077−33084.
29. Dickerson, R. E., and Geis, I. (1983) *Hemoglobin: Structure, Function, Evolution, and Pathology*, Benjamin/Cummings Publishing Co., Inc., Menlo Park, CA.
30. Kavanaugh, J. S., Rogers, P. H., Case, D. A., and Arnone, A. (1992) *Biochemistry 31*, 4111−4121.
31. Kavanaugh, J. S., Weydert, J. A., Rogers, P. H., and Arnone, A. (1998) *Biochemistry 37*, 4358−4373.
32. Kavanaugh, J. S., Chafin, D. R., Arnone, A., Mozzarelli, A., Rivetti, C., Rossi, G. L., Kwiatkowski, L. D., and Noble, R. W. (1995) *J. Mol. Biol. 248*, 136−150.
33. Kavanaugh, S. J., Weydert, J. A., Rogers, P. H., Arnone, A., Hui, H. L., Wierzba, A. M., Kwiatkowski, L. D., Paily, P., Noble, R. W., Bruno, S., and Mozzarelli, A. (2001) *Protein Sci. 10*, 1847−1855.
34. Mozzarelli, A., Rivetti, C., Rossi, G. L., Eaton, W. A., and Henry, E. R. (1997) *Protein Sci. 6*, 484−489.

BI010988P